Journal of Sustainable Construction Materials and Technologies

Volume 11 | Issue 2 Article 10

Sustainable High-Density Polyethylene Composites Reinforced with Olive Pomace: Production and Characterization

Recai Arslan

Düzce University, Recycling of Agricultural Wastes to Industry Application and Research Center, 81620, Düzce, Türkiye, recaiarslan@duzce.edu.tr

Azime Subaşi

Düzce University, Gümüşova Vocational School, Department of Metalurgy, 81850, Düzce, Türkiye

Follow this and additional works at: https://commons.yildiz.edu.tr/jscmt

Recommended Citation
Arslan, Recai and Subaşi, Azime (2026) "Sustainable High-Density Polyethylene Composites Reinforced with Olive Pomace: Production and Characterization," *Journal of Sustainable Construction Materials and Technologies*: Vol. 11: Iss. 2, Article 10.
https://doi.org/10.29187/2458-973X.1226
Available at: https://commons.yildiz.edu.tr/jscmt/vol11/iss2/10

This Research Article is brought to you for free and open access by YTU Press. It has been accepted for inclusion in Journal of Sustainable Construction Materials and Technologies by an authorized editor of YTU Press.

JOURNAL OF SUSTAINABLE CONSTRUCTION MATERIALS AND TECHNOLOGIES 2026;11:369–380

Scan the QR to view the full-text article on the journal website

RESEARCH ARTICLE

Sustainable High-Density Polyethylene Composites Reinforced with Olive Pomace: Production and Characterization

Recai Arslan [a,*], **Azime Subaşi** [b]

[a] Düzce University, Recycling of Agricultural Wastes to Industry Application and Research Center, 81620, Düzce, Türkiye
[b] Düzce University, Gümüşova Vocational School, Department of Metalurgy, 81850, Düzce, Türkiye

ABSTRACT

In this study, olive pomace (OP), an abundant agro-industrial by-product, was incorporated into a high-density polyethylene (HDPE) matrix at loadings of 0–20 wt.% to develop sustainable polymer composites. The influence of OP loading on the physical, mechanical, structural, and thermal properties of the composites was systematically investigated. Increasing OP loading resulted in elevated moisture content and water absorption, attributed to the hydrophilic nature of the lignocellulosic filler. Composite density and Shore D hardness exhibited a progressive increase with OP loading. In contrast, tensile and impact properties remained statistically not significantly changed at 5 wt.% OP loading, while higher filler loadings (10–20 wt.%) resulted a significant decrease in mechanical performance, accompanied by a transition from ductile to more brittle fracture behavior. Fourier-transform infrared spectroscopy (FTIR) analysis indicated a decrease in the intensity of characteristic HDPE bands and partial disruption of polymer crystallinity, suggesting predominantly physical interactions between the matrix and filler. Thermogravimetric analysis (TGA) revealed a decrease in the onset degradation temperature with OP addition; however, enhanced char formation contributed to improved thermal stability at higher degradation stages. Overall, the findings suggest that OP is more suitable for use in HDPE composites at relatively low filler loadings.

Keywords: Olive pomace, HDPE composites, Mechanical properties, Thermal stability, Sustainable materials

1. Introduction

The increasing global population, growing sustainability concerns, and the depletion of fossil-based resources have intensified the demand for environmentally friendly and innovative materials across various industrial sectors [1, 2]. In recent years, bio-based composites, which are innovative materials produced from renewable raw resources, have attracted considerable attention as an effective approach to reducing the environmental impacts of conventional plastics, particularly in the composites industry [3, 4]. These materials, reinforced with plant-derived fillers, are valued for their low density, cost-effectiveness, ease of processing, and favorable thermal and acoustic insulation properties [5]. Bio-based composites are increasingly replacing synthetic alternatives in fields such as construction, automotive, aerospace, and electronics [6–8].

Plastic materials are widely used in numerous industrial applications, including textiles, construction, food packaging, and the medical sector, owing to their low cost, lightweight nature, versatile processability, and high chemical stability [9]. Global plastic production has exceeded 300 million metric tons annually, raising significant environmental concerns due to the persistence and low biodegradability of plastics [10]. In this context, the development of

Received 27 February 2026; revised 21 May 2026; accepted 18 June 2026.
Available online 26 June 2026

* Corresponding author.
E-mail address: recaiarslan@duzce.edu.tr (R. Arslan).

https://doi.org/10.29187/2458-973X.1226
2458-973X/© 2026 Published by Yıldız Technical University Press, İstanbul, Türkiye. This is an open access article under the CC BY-NC 4.0 Licence (https://creativecommons.org/licenses/by-nc/4.0/).

sustainable and environmentally friendly polymer-based materials has attracted increasing attention.

Thermoplastic polymers-including polyethylene (PE), polypropylene (PP), polyvinyl chloride (PVC), polystyrene (PS), polymethyl methacrylate (PMMA), and polyamide (PA) are widely used in composite manufacturing. PE is particularly preferred due to its low cost, high processability via extrusion and injection molding, mechanical robustness, and excellent chemical resistance [2, 11]. In recent years, the addition of bio-based fillers into thermoplastic matrices has emerged as an effective approach to reduce environmental impact while maintaining acceptable material performance. Plant-based fillers are considered promising alternatives to synthetic reinforcements due to their low environmental footprint, low density, renewability, and favorable mechanical properties [12]. Besides natural fibers such as hemp, jute, sisal, and bamboo, different agricultural wastes, including hazelnut, walnut, almond, and pistachio shells have also been investigated as particulate fillers in polymer composites [13–18]. The utilization of agricultural by-products with high waste generation potential in composite production not only contributes to waste valorization and resource efficiency but also supports the development of sustainable composite materials with reduced environmental effects [19].

Olive pomace (OP), composed of pits, skins, and pulp remaining after olive oil extraction, stands out as a promising lignocellulosic filler due to its high cellulose-hemicellulose-lignin content, low cost, and chemical functionality [20–22]. Chemically, OP contains cellulose (8–23%), hemicellulose (9–24%), lignin (21–42%), and a high amount of extractives (>30%), depending on the olive variety and processing conditions [23, 24]. Although traditionally used as fuel, feed additive, activated carbon precursor, or pellet raw material, OP has recently attracted growing interest for bioplastic and biocomposite applications [25, 26].

Recent studies have increasingly focused on the utilization of agricultural and agro-industrial wastes as reinforcing agents in thermoplastic composites in order to improve sustainability and reduce environmental burdens associated with synthetic fillers [27]. Numerous lignocellulosic wastes, including rice husk, wood flour, wheat straw, coconut shell, almond shell, hazelnut shell, and olive-derived by-products, have been incorporated into polymer matrices such as PP, PE, PLA, PVC, and epoxy systems [28–32]. These studies demonstrated that natural fillers can significantly influence the mechanical, thermal, rheological, and physical properties of composites depending on filler morphology, particle size, interfacial adhesion, and dispersion quality [33]. In particular, agricultural waste-based composites have been reported to offer advantages such as low density, renewability, biodegradability, reduced material cost, and a lower carbon footprint compared with conventional petroleum-based composites [34, 35]. Furthermore, the valorization of olive industry wastes has gained increasing attention due to the large quantities of waste generated annually in Mediterranean countries and the environmental concerns associated with their disposal [36, 37].

Studies investigating OP-filled polymer composites have demonstrated that the resulting material properties depend on the polymer matrix, filler loading, and processing conditions. High filler ratios in polyester and polystyrene matrices, for example, have been shown to reduce yield stress, elastic modulus, and overall mechanical integrity, largely due to agglomeration and weak interfacial bonding [37–39]. Similar decreases in tensile strength, elongation at break, impact resistance, and elastic modulus have been reported for high-density polyethylene (HDPE), low-density polyethylene (LDPE), and polyvinyl chloride (PVC) matrices containing OP [40]. These negative effects are generally attributed to insufficient matrix-filler compatibility and restricted polymer chain mobility at high filler contents [33].

Conversely, several studies demonstrate that OP can enhance mechanical, thermal, or thermo-mechanical performance when utilized under suitable conditions. Improvements in thermal stability and Young's modulus have been observed in polypropylene-OP composites [30], while PLA-based systems have shown increased stiffness with varying particle sizes of OP [41]. Furthermore, OP addition into modified recycled PP has been shown to increase both flexural and tensile modulus [26], and similar enhancements in Vicat softening point, heat distortion temperature, and tensile strength have also been reported in multiple polymer matrices [14, 18, 21, 28].

Despite the increasing number of studies on natural fiber- and agricultural waste-reinforced thermoplastics, comprehensive investigations focusing specifically on OP-filled HDPE composites remain limited [36]. Most previous studies primarily concentrated on selected mechanical properties or thermal behavior, while integrated evaluations combining physical, chemical, thermal, and mechanical characterization are still scarce. In addition, inconsistencies in the reported findings regarding the effect of OP loading on composite performance indicate the need for systematic optimization studies. Therefore, further research is required to better understand the structure-property relationships of OP-reinforced

HDPE composites and to determine suitable filler contents for sustainable industrial applications.

In this study, OP was incorporated into an HDPE matrix at 5, 10, 15, and 20% by weight to produce bio-based composites. The resulting materials were extensively characterized in terms of moisture content, water absorption, density, hardness, tensile strength, impact strength, Fourier-transform infrared spectroscopy (FTIR), and thermogravimetric analysis (TGA). This comprehensive approach aims to elucidate the structure-property relationships of HDPE- OP composites and to evaluate the influence of different OP addition levels on composite performance for sustainable material development.

2. Materials and method

2.1. Materials

The HDPE used in this study was supplied by Altan Plastik (İstanbul, Türkiye). Its technical specifications are as follows: density of 0.946 g/cm^3, melt flow index of 6.0 g/10 min (190 °C/21.6 kg), tensile strength at yield of 24.0 MPa, tensile strain at break greater than 600%, flexural modulus of 1000 MPa, and a processing temperature range of 190–240 °C for blow molding.

The OP used as the lignocellulosic filler was obtained from Tıngır Olive Oil Factory (Sakarya, Türkiye). This by-product consists of a mixture of olive pits, husks, skins, and small fragments of leaves and branches. The OP was first dried in a vacuum oven at 105 °C for 24 h. The dried material was subsequently ground using a Wiley-type mill (Retsch SM 100) and fractionated with a laboratory shaker sieve (Retsch AS 200). The moisture content of the fraction retained on the 40-mesh sieve was determined in accordance with ASTM D4442M-20 [42].

2.2. Composite production

Composite production was conducted in accordance with the mixture ratios provided in Table 1, and the resulting formulations were coded accordingly. In the preparation stage, powdered OP and HDPE granules were premixed and subsequently compounded in a twin-screw extruder operating at a screw speed of 40 rpm, under a processing pressure of 30 bar, and at a temperature profile ranging from 170 to 200 °C. Upon completion of the compounding process, the extrudates were dried at 105 °C to ensure the removal of residual moisture prior to molding.

Table 1. Sample codes and formulation compositions of OP-reinforced HDPE composites.

Composite code	HDPE (wt.%)	OP (wt.%)
HDPE-OP-0 (control)	100	0
HDPE-OP-5	95	5
HDPE-OP-10	90	10
HDPE-OP-15	85	15
HDPE-OP-20	80	20

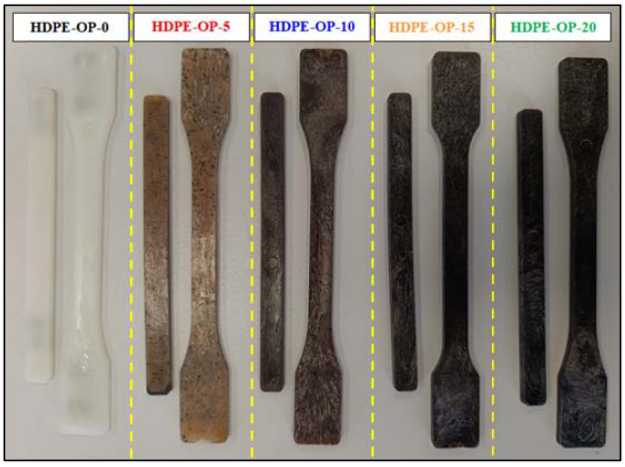

Fig. 1. OP-reinforced HDPE composites.

The dried materials were then shaped into test specimens using an injection molding machine, with specimen dimensions conforming to the ISO 527-2 [43] standard (Fig. 1). During injection molding, the melt temperature was controlled within the range of 170–200 °C, while the screw speed was set to 45 rpm. For compression molding applications, a processing temperature of 170 °C and a pressure of 100 bar were employed.

2.3. Testing and characterization of composites

2.3.1. Physical properties

The moisture content of the composite samples was determined in accordance with ASTM D4442M-20 [42], density was measured following ASTM D792-20 [44], hardness (Shore D) was evaluated according to ASTM D2240-15 [45], and water absorption was assessed in compliance with ASTM D570-98 [46]. All physical test results are given as the average of at least three samples.

2.3.2. Mechanical properties

Tensile tests were conducted using a BESMAK universal testing machine in accordance with the ISO 527-2 [43] standard. The impact strength was determined using a notched Charpy impact tester (XJJ-50W) in accordance with ISO 179-1 [47]. During the test, the pendulum energy was set to 7.5 J, and the impact speed was 3.8 m/s. All mechanical test results are given as the average of at least three samples.

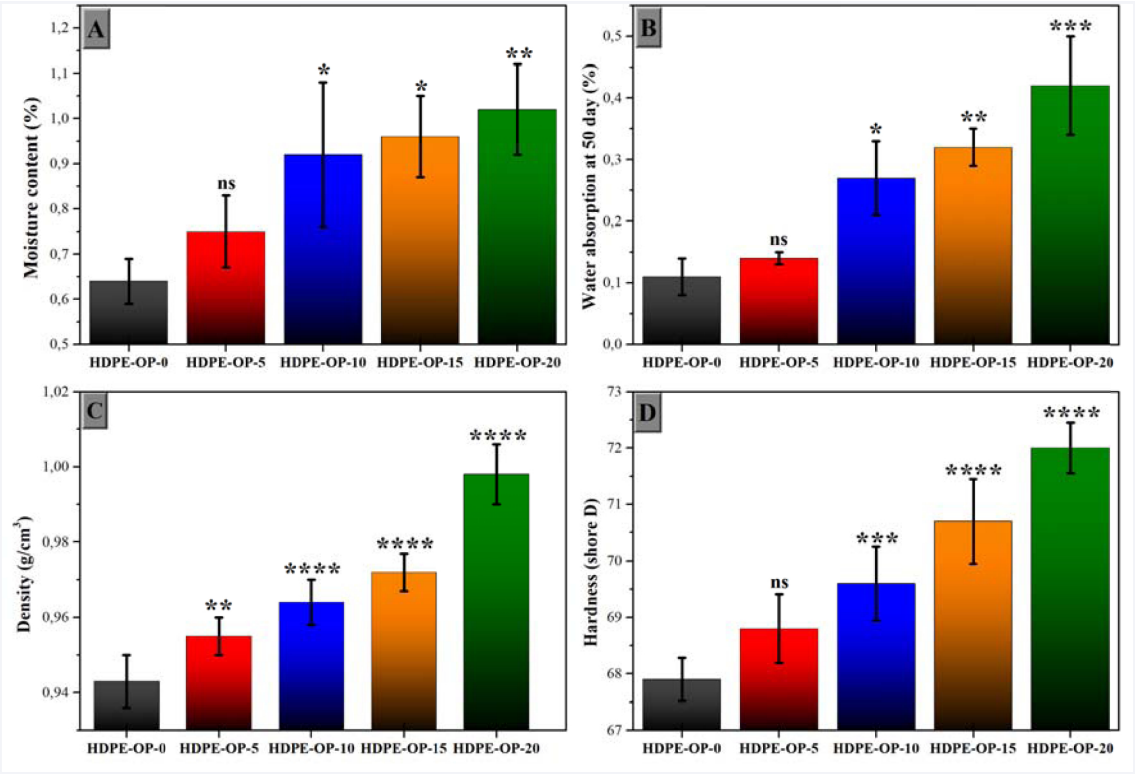

Fig. 2. Physical properties of OP-reinforced HDPE composites: (a) Moisture content, (b) water absorption at 50 days, (c) density, and (d) hardness (shore D). Different lowercase letters indicate significant differences among groups. Statistical significant levels are expressed as ****P < 0.0001, ***P < 0.001, **P < 0.01, *P < 0.05, and ns: not significant.

2.3.3. Fourier-transform infrared (FTIR) spectroscopy analysis

FTIR spectra were recorded using an IRPrestige-21 FT-IR spectrophotometer (BRUKER, ALPHA model) equipped with a single-reflection ATR sampling module. Spectra were collected at a resolution of 4 cm^{-1} in the 400–4000 cm^{-1} wavenumber range, averaging 32 scans. The spectral data were analyzed using the Gaussian curve-fitting method in OriginPro 2013 (OriginLab Corporation, Northampton, MA, USA). Optimal Gaussian fits were selected for four characteristic bands, where the reduced chi-square values were $< 1\times10^{-6}$ and the coefficients of determination (R^2) ranged between 0.94 and 0.96.

2.3.4. Thermogravimetric (TGA) analysis

Thermogravimetric analysis (TGA) was performed using a HITACHI STA7300 instrument under a nitrogen atmosphere, with a heating rate of 20 °C/min from room temperature up to 800 °C.

2.3.5. Statistical analysis

Statistical analysis was performed using one-way analysis of variance (ANOVA) in GraphPad Prism 6 (GraphPad Software, USA) to evaluate differences in moisture content, water absorption, density, hardness (Shore D), tensile strength, elongation at break, and impact strength of the composites. Mean comparisons were conducted using Tukey's multiple comparison test at a significance level of $P < 0.05$.

3. Results and discussion

3.1. Physical properties of OP-reinforced HDPE composites

The moisture content, water absorption (at 50 days), density, and Shore D hardness values of OP-reinforced HDPE composites are presented in Fig. 2, while their water absorption behavior on different days is presented in Fig. 3.

The moisture content of the HDPE-OP-0 composite was 0.64%, while the addition of 5, 10, 15, and 20 wt.% OP increased the moisture content to 0.75% (ns), 0.92% ($P < 0.05$), 0.96% ($P < 0.05$), and 1.02% ($P < 0.01$), respectively (Fig. 2A). A similar trend was observed for water absorption. After 50 days of soaking in water, the water absorption of the HDPE-OP-0 remained limited to 0.11%, while the values for HDPE-OP-5, HDPE-OP-10, HDPE-OP-

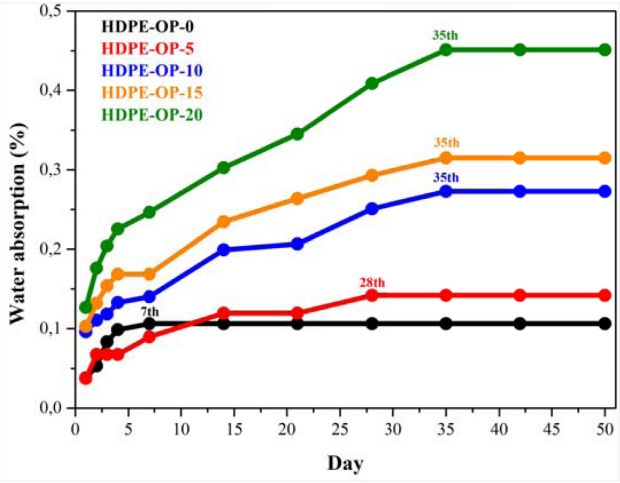

Fig. 3. Water absorption behavior of OP-reinforced HDPE composites after 50 days of soaking in water.

15, and HDPE-OP-20 increased to 0.14% (ns), 0.27% ($P < 0.05$), 0.32% ($P < 0.01$), and 0.42% ($P < 0.001$), respectively (Fig. 2B).

The saturation time also varied depending on OP loading. Water absorption reached equilibrium on day 7 for HDPE-OP-0, day 28 for HDPE-OP-5, and approximately day 35 for composites containing 10 wt.% OP and above (Fig. 3). The progressive delay in equilibrium with increasing OP loading indicates enhanced moisture diffusion and retention within the composite structure.

Both moisture content and water absorption increased systematically with increasing OP loading, consistent with previous studies [28]. This behavior is mainly attributed to the addition of hydrophilic OP into the inherently hydrophobic HDPE matrix. The lignocellulosic structure of OP, rich in hydroxyl groups, promotes hydrogen bonding with water molecules, thereby facilitating moisture uptake and swelling within the filler phase. Moisture absorption continues until equilibrium is reached, resulting in mass gain and possible dimensional changes [48]. In addition to the chemical nature of the filler, the formation of interfacial voids and microdefects at the matrix–filler interface likely further contributes to the observed increase in water uptake. Similar observations were reported by Kuzmin et al. [49], who demonstrated that the addition of hydrophobic waste rubber reduced moisture absorption in HDPE/barley straw composites, emphasizing the dominant role of filler chemistry in moisture-related behavior. Although increasing OP loading adversely affected water resistance, the overall water absorption values remained relatively low (<0.5% after 50 days), suggesting that the composites may still be suitable for indoor or semi-protected applications where prolonged direct moisture exposure is limited.

The density of the HDPE-OP-0 composite was 0.943 g/cm^3, while the addition of 5, 10, 15, and 20 wt.% OP increased the density to 0.955 g/cm^3 ($P < 0.01$), 0.964 g/cm^3 ($P < 0.0001$), 0.972 g/cm^3 ($P < 0.0001$), and 0.998 g/cm^3 ($P < 0.0001$), respectively (Fig. 2C). A progressive increase in density was observed with OP loading, with density increases of 1.28%, 2.22%, 3.01%, and 5.75% for the composites containing 5, 10, 15, and 20 wt.% OP, respectively. This trend is consistent with the findings of Tuna and Şen [50], who reported a 3.62% increase in density following the addition of 10% OP into LDPE composites. The gradual increase in density indicates that OP can contribute to the production of more compact composite structures, which may be advantageous in applications requiring improved rigidity and dimensional stability.

The hardness (Shore D) of the HDPE-OP-0 composite was 67.9, while the addition of 5, 10, 15, and 20 wt.% OP increased the hardness to 68.8 (ns), 69.6 ($P < 0.001$), 70.7 ($P < 0.0001$), and 72.0 ($P < 0.0001$), respectively (Fig. 2D). A progressive increase in hardness was observed with increasing OP loading, with improvements of 1.33%, 2.50%, 4.12%, and 6.04% for the composites containing 5, 10, 15, and 20 wt.% OP, respectively. Similar results were reported by Tuna and Şen [50], who observed a 7.48% increase in hardness in LDPE composites reinforced with 10% olive mill waste. In contrast, Anaç et al. [51] reported a 9.71% decrease in hardness following the addition of 10% OP into a PLA matrix. This discrepancy highlights the determining role of the polymer matrix chemistry and filler-matrix interfacial interactions on composite hardness. The increased hardness observed in the present study suggests that OP addition may improve surface resistance and rigidity, potentially supporting the use of these composites in non-structural applications such as interior panels, decking components, and wood-plastic composite products where enhanced surface hardness is desirable.

3.2. Mechanical properties of OP-reinforced HDPE composites

The tensile strength and elongation at break values of OP-reinforced HDPE composites are presented in Fig. 4, while the corresponding tensile stress-strain curves are shown in Fig. 5.

The tensile strength of the HDPE–OP–0 composite was 21.2 MPa, while the addition of 5, 10, 15, and 20 wt.% OP decreased the tensile strength to 20.6 MPa (ns), 14.6 MPa ($P < 0.0001$), 9.39 MPa ($P < 0.0001$),

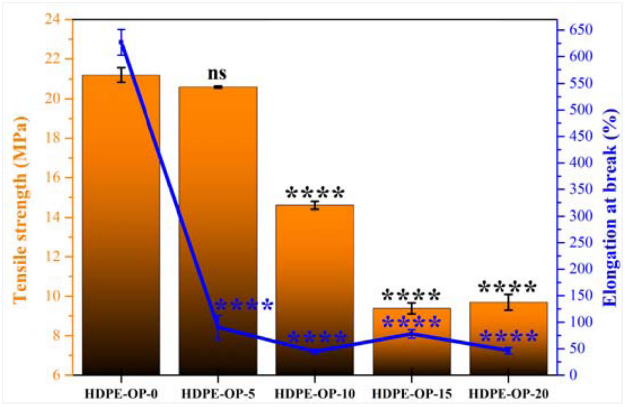

Fig. 4. Tensile strength-elongation at break values of OP-reinforced HDPE composites. Different lowercase letters indicate significant differences among groups. Statistical significant levels are expressed as ****P < 0.0001, ***P < 0.001, **P < 0.01, *P < 0.05, and ns: not significant.

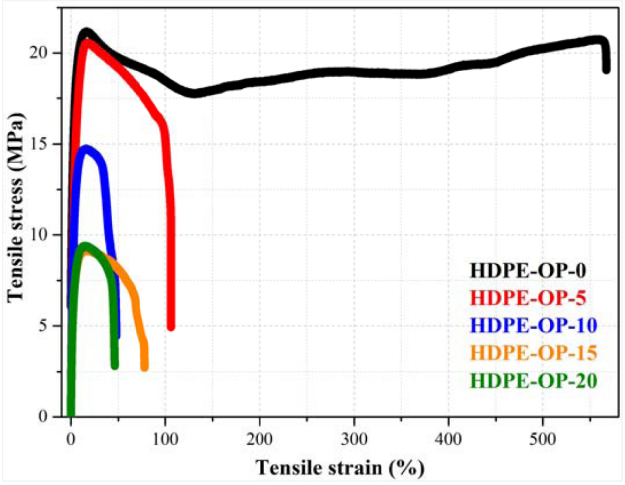

Fig. 5. Tensile stress-strain curves of OP-reinforced HDPE composites.

and 9.70 MPa (P < 0.0001), respectively (Fig. 4). The tensile strength decreased progressively with increasing OP loading, corresponding to decreases of 2.83%, 31.1%, 55.7%, and 54.2% relative to the control composite.

The elongation at break of the HDPE–OP–0 composite was 626.8%, while the addition of 5, 10, 15, and 20 wt.% OP decreased the elongation at break to 90.1% (P < 0.0001), 44.9% (P < 0.0001), 78.1% (P < 0.0001), and 46.2% (P < 0.0001), respectively (Fig. 4). Overall, increasing OP loading resulted in a pronounced decrease in both tensile strength and elongation at break. The decrease in tensile strength can be attributed to the weak interfacial adhesion between the OP particles and the HDPE matrix [52]. Magalhães et al. [53] similarly reported that OP particles primarily behave as fillers rather than reinforcing agents in polymer matrices. Likewise, decreases in tensile strength have been associated with insufficient wetting of OP particles, particle agglomeration, and weak interfacial adhesion between the filler and polymer matrix [54, 55]. Although a relatively uniform dispersion of filler particles may help minimize agglomeration-induced stress concentrations, effective dispersion alone is not sufficient to ensure improved mechanical performance. In the absence of strong interfacial bonding, stress transfer from the polymer matrix to the filler phase becomes ineffective, leading to interfacial debonding, fiber pull-out, and the initiation of microcracks under tensile loading [56, 57]. Consequently, the reinforcing efficiency of the lignocellulosic filler is significantly reduced. Such decreases in tensile strength are commonly reported in lignocellulosic filler-hydrophobic polymer systems due to the inherent incompatibility between the hydrophilic filler surface and the nonpolar polymer matrix [58].

Examination of the tensile stress-strain curves presented in Fig. 5 further supports these findings. The neat HDPE exhibited typical ductile behavior with high deformation capacity, while increasing OP loading resulted in a transition toward more brittleness. This change is mainly related to the inherently rigid and brittle nature of lignocellulosic OP particles [59]. Moreover, the increase in hardness (Shore D) values observed with higher OP loadings (Fig. 2D) is consistent with the decreased ductility and increased brittleness of the composites.

The impact strength values of OP-reinforced HDPE composites are presented in Fig. 6. The Charpy impact strength of the HDPE-OP-0 was measured as 40.4 kJ/m^2. The addition of 5 wt.% OP resulted in a slight increase in impact strength of 8.66% (ns), indicating that low filler loading does not significantly alter the energy absorption capability of the matrix. However, this change is statistically not significant, suggesting that the observed increase should be interpreted as a minor fluctuation rather than a meaningful improvement in toughness. In contrast, further increases in OP loading to 10, 15, and 20 wt.% led to substantial decreases in impact strength of 20.5% (P < 0.001), 22.8% (P < 0.001), and 32.7% (P < 0.0001), respectively. These results indicate that the impact resistance of the composites deteriorates beyond low filler loadings, highlighting a filler-loading-dependent transition in dynamic mechanical performance. A similar trend has been reported by Banat et al. [14], who observed a decrease in impact strength upon exceeding 5 wt.% OP addition in HDPE-based composites. This behavior

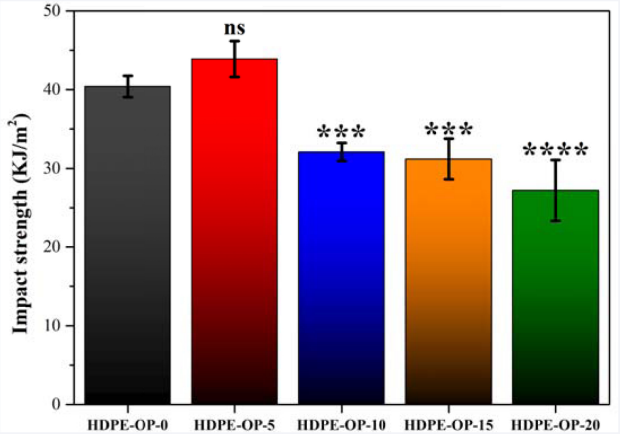

Fig. 6. Impact strength values of OP-reinforced HDPE composites. Different lowercase letters indicate significant differences among groups. Statistical significant levels are expressed as ****P < 0.0001, ***P < 0.001, **P < 0.01, *P < 0.05, and ns: Not significant.

was associated with changes in the energy dissipation mechanisms under impact loading and increased restriction of plastic deformation. In comparison, LDPE-based composites reinforced with OP exhibited a more pronounced sensitivity to filler addition, with impact strength decreases of 58.2% and 72.1% reported at OP loadings of 5 and 10 wt.%, respectively [50]. Consistent findings were also presented by Jurado-Contreras et al. [26], who associated the progressive decline in impact strength with increasing OP loading to insufficient interfacial interaction between the polymer matrix and OP particles and limiting efficient stress transfer during dynamic loading. Furthermore, Naghmouchi et al. [3] demonstrated that rigid filler particles can act as stress concentration sites within the polymer matrix, reducing crack initiation energy and promoting premature interfacial debonding, ultimately leading to inferior impact performance.

Overall, the mechanical results indicate that OP acts primarily as a particulate filler rather than a reinforcing agent in the HDPE matrix, with its effectiveness strongly dependent on loading level. While high filler loadings significantly compromise tensile and impact performance due to interfacial limitations, low-to-moderate additions can still be considered for applications where moderate mechanical requirements are acceptable. In this context, the present findings suggest that HDPE–OP composites may be suitable for non-load-bearing and semi-structural applications, particularly in products where sustainability, cost reduction, and waste valorization are prioritized over high mechanical strength. However, the use of untreated OP also defines the practical scope of these composites in terms of performance limitations.

3.3. FTIR analysis of OP-reinforced HDPE composites

The FTIR spectra of OP-reinforced HDPE composites are presented in Fig. 7, and the percentage changes in selected band intensities are summarized in Table 2. Characteristic vibrations belonging to CH_2 groups are clearly observed in the spectrum of pure HDPE. Accordingly, the intense bands at 2911 and 2846 cm^{-1} correspond to the asymmetric and symmetric stretching vibrations of methylene (CH_2) groups, the band at 1467 cm^{-1} corresponds to the CH_2 bending vibration, and the band at 718 cm^{-1} corresponds to the CH_2 rocking vibration, which is an indicator of the crystalline phase of HDPE [60, 61].

Due to the dispersion of OP particles within the HDPE matrix, the characteristic bands of lignocellulosic components (cellulose, hemicellulose, and lignin) were largely masked by the strong CH_2 bands of HDPE. However, with increasing OP loading, a clear decrease in the intensities of all major HDPE bands was observed. In the HDPE-OP-20 sample containing 20% OP, the band areas at 2911, 2846, 1467, and 718 cm^{-1} decreased by 45.9%, 45.7%, 43.3%, and 42.4%, respectively, compared to HDPE-OP-0 (Table 2). This decrease can be attributed to the physical disruption of the ordered packing of HDPE chains by the OP particles, and the presence of weak van der Waals interactions between the hydrophilic functional groups of OP and the hydrophobic HDPE matrix [30, 60].

The decrease in the intensity of bands at 1467 cm^{-1} and 718 cm^{-1} suggests a partial decrease in the crystalline ordering of HDPE chains, indicating a transition toward a more disordered structure with increasing filler loading [62]. This structural modification is consistent with the mechanical results, particularly the decrease in ductility at higher OP loadings. In addition, the emergence and progressive intensification of absorption bands in the 1500–1730 cm^{-1} region with increasing OP loading indicates the gradual addition of lignocellulosic constituents into the HDPE matrix, despite their relatively low intensity due to the dominant spectral contribution of HDPE. The bands observed in this region are mainly attributed to C=O stretching vibrations associated with ester, carboxylic acid, and ketone functionalities present in hemicellulose and lignin fractions, as well as to C=C and conjugated C=O vibrations originating from aromatic structures. These assignments are consistent with previously reported FTIR characteristics of lignocellulosic biomass, where hemicellulose- and lignin-derived carbonyl groups typically appear in the 1730–1740 cm^{-1} region due to acetyl and uronic ester

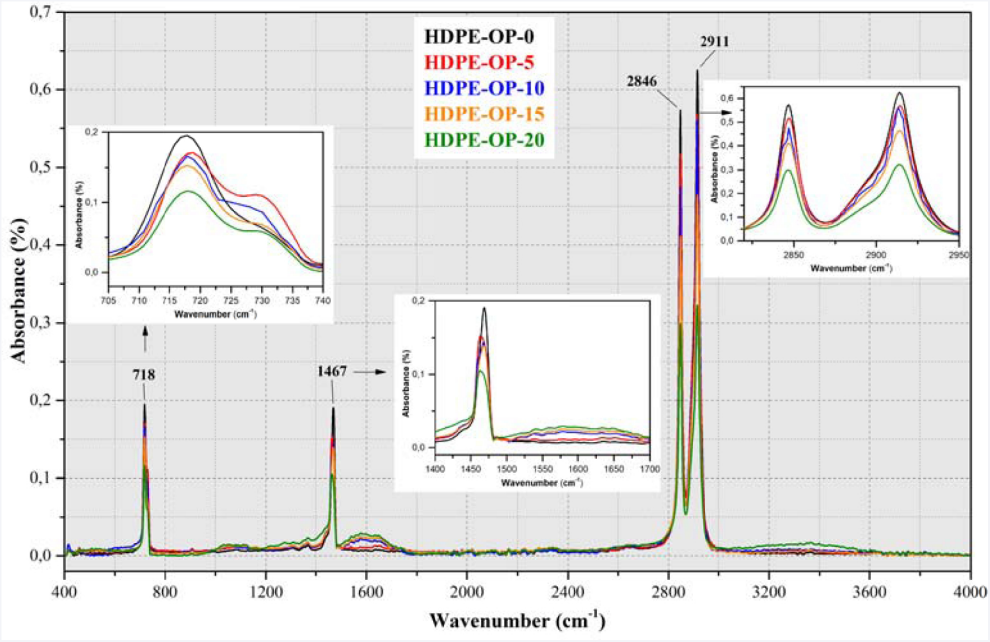

Fig. 7. FTIR spectra of OP-reinforced HDPE composites.

Table 2. Peak intensity (%) of OP-reinforced HDPE composites at different wavelengths.

	Peak intensity (%)			
Composite type	718 cm^{-1}	1467 cm^{-1}	2846 cm^{-1}	2911 cm^{-1}
HDPE-OP-0 (control)	23.1	24.1	24.7	24.6
HDPE-OP-5	23.5	22.3	23.2	23.2
HDPE-OP-10	21.5	21.0	20.2	20.5
HDPE-OP-15	18.7	19.0	18.5	18.4
HDPE-OP-20	13.3	13.6	13.4	13.3

functionalities in hemicellulose and lignin structures [63, 64]. Moreover, OP wastes are known to contain significant amounts of lignin, hemicellulose, and residual lipidic compounds, which also contribute to carbonyl-related absorptions in this spectral region [40]. In particular, FTIR studies on OP-based composites have similarly reported the presence of absorption bands around 1730–1750 cm^{-1}, attributed both to lignocellulosic carbonyl functionalities and residual oil-derived components within the biomass structure [64]. Therefore, the systematic increase in the intensity of these bands with increasing OP loading confirms the successful addition and dispersion of the lignocellulosic filler within the HDPE matrix and is fully consistent with the intrinsic chemical composition of OP reported in the literature [65]. Overall, FTIR results confirm that the interaction between HDPE and OP is predominantly physical, indicating limited interfacial compatibility without chemical bonding, which plays a key role in the observed mechanical performance.

3.4. TGA analysis of OP-reinforced HDPE composites

The thermogravimetric (TGA) curves of OP-reinforced HDPE composites are presented in Fig. 8, while the corresponding TGA data are summarized in Table 3. All samples exhibited thermal stability up to approximately 300 °C, after which a single dominant degradation stage was observed. This behavior indicates that the thermal decomposition of the composites is mainly governed by the HDPE matrix, with the lignocellulosic fraction influencing the early degradation stage [66].

The temperature at 5% weight loss ($T_{5\%}$) for neat HDPE was 463 °C. With the addition of OP at 5, 10, 15, and 20 wt.%, $T_{5\%}$ values decreased to 459, 427, 420, and 350 °C, respectively. This decrease is attributed to the lower thermal stability of lignocellulosic components, particularly cellulose and hemicellulose, which initiate degradation at relatively lower temperatures (350–440 °C) [66, 67]. This

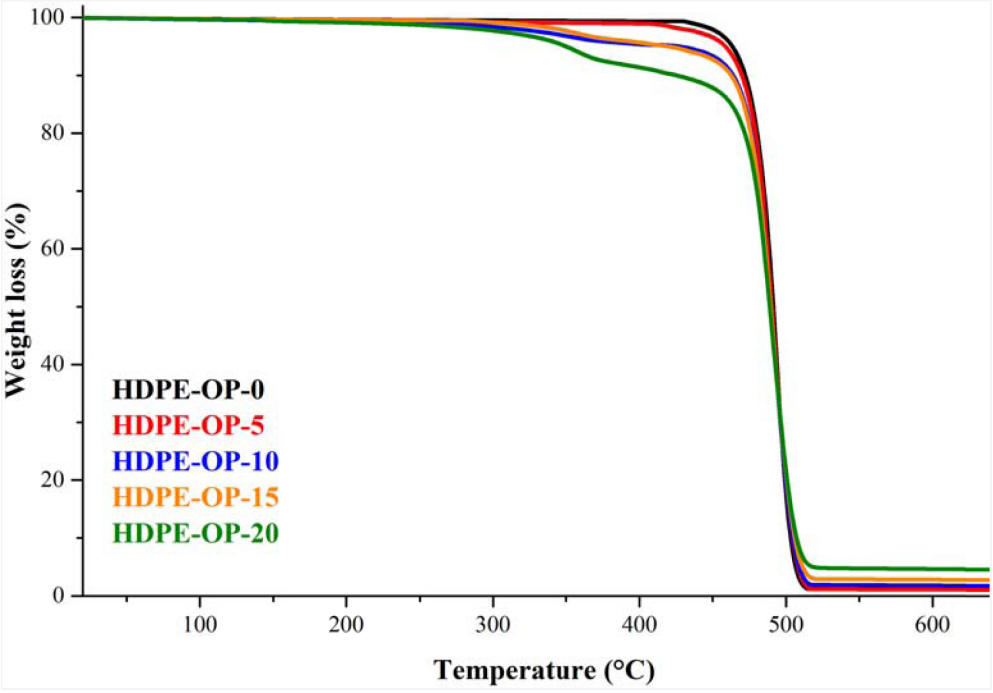

Fig. 8. TGA curve of OP-reinforced HDPE composites.

Table 3. TGA data (%) of OP-reinforced HDPE composites.

Composite type	$T_{5\%}$	$T_{95\%}$	Total weight loss (%) 600 °C
HDPE-OP-0 (control)	463	507	98.8
HDPE-OP-5	459	508	98.8
HDPE-OP-10	427	509	98.2
HDPE-OP-15	420	511	97.2
HDPE-OP-20	350	518	95.3

$T_{5\%}$: Temperature value at 5% weight loss, $T_{95\%}$: Temperature value at 95% weight loss.

indicates that OP loading slightly reduces the initial thermal resistance of the composites, thereby narrowing the safe processing/thermal stability window at high filler loadings.

In contrast, the temperature corresponding to 95% weight loss ($T_{95\%}$) increased with increasing OP loading. While HDPE exhibited a $T_{95\%}$ value of 507 °C, the composites containing 5, 10, 15, and 20 wt.% OP showed values of 508, 509, 511, and 518 °C, respectively. This improvement at higher degradation stages is attributed to the formation of thermally stable char residues derived from the lignin-rich structure of OP, which acts as a protective barrier during thermal decomposition.

Consistently, total weight loss at 600 °C decreased from 98.8% (HDPE-OP-0) to 95.3% (HDPE-OP-20), while residual char content increased with OP loading. This trend confirms the contribution of lignin-derived aromatic structures to char formation, enhancing thermal resistance at elevated temperatures [54]. From an application perspective, these results suggest that although OP reduces the initial thermal stability of HDPE composites, it improves char yield and high-temperature resistance, which may be advantageous in applications where thermal barrier properties are more critical than initial degradation temperature.

4. Conclusion

This study systematically investigated the effects of OP addition on the physical, mechanical, structural, and thermal properties of HDPE-based composites, highlighting the role of OP loading in governing the overall composite performance.

The addition of OP increased moisture content and water absorption, accompanied by delayed saturation times, which were primarily attributed to the hydrophilic nature of the lignocellulosic structure. Density and Shore D hardness values increased steadily with higher OP loadings, reflecting the rigid and dense nature of the filler and indicating improved surface resistance and dimensional rigidity.

Mechanical performance exhibited a filler-loading-dependent behavior. A low OP loading (5 wt.%) showed a statistically not significant effect on impact strength, indicating that limited filler addition does not substantially alter the energy absorption

capability of the HDPE matrix. However, further increases in OP loading resulted in a pronounced decrease in tensile and impact strength, which was mainly attributed to insufficient interfacial adhesion between the HDPE matrix and OP particles, limiting effective stress transfer under applied loading.

FTIR analysis confirmed that the interactions between HDPE and OP were predominantly physical, resulting in limited interfacial compatibility and partial disruption of HDPE crystallinity. Thermogravimetric analysis revealed that although the onset degradation temperature decreased with OP addition, enhanced char formation improved thermal resistance at higher degradation stages, suggesting a potential thermal barrier effect at elevated temperatures.

From an application perspective, the overall results indicate that HDPE–OP composites are more suitable for non-load-bearing and semi-structural applications where moderate mechanical performance, improved hardness, and sustainability considerations are prioritized over high strength requirements. Potential application areas include interior panels, packaging components, decking materials, and wood-plastic composite alternatives. However, the applicability of these materials is limited to low-to-moderate filler loadings and untreated OP, which defines the practical scope of their performance in real-world applications. In addition, future studies involving detailed life cycle assessment (LCA) analyses may provide further insight into the environmental benefits, carbon footprint reduction potential, and overall sustainability performance of OP-based composite systems. From a future perspective, surface modification of OP and the addition of compatibilizers are expected to significantly enhance interfacial bonding, potentially enabling higher filler contents without severe mechanical deterioration and thereby broadening their industrial usability within sustainable composite systems.

Acknowledgement

The authors would like to acknowledge Altan Plastik (İstanbul, Türkiye) for their contributions and support in the composite production carried out in this study.

Ethics

There are no ethical issues with the publication of this manuscript.

Conflict of interest

The authors declared no potential conflicts of interest with respect to the research, authorship, and/or publication of this article.

Author's contributions

Author #1 Recai & Arslan: Conception, Design, Supervision, Materials, Data Collection, Analysis, Literature Review, Writer, Critical Review.

Author #2 Azime & Subaşı: Conception, Design, Supervision, Data Collection.

Funding

The authors received no financial support for the research, authorship, and/or publication of this article.

Data availability statement

All graphs and data obtained or generated during the investigation appear in the published article.

References

1. Kalia S, Kaith BS, Kaur I. Cellulose fibers: Bio- and nano-polymer composites. Green Chemistry and Technology, Springer; 2011.
2. Lim KM, Khoo V, Ong WJ. Trash-to-energy: Shedding light on plastic and biomass valorization through artificial photosynthesis towards sustainability. *Exploration*. 2025;5(6):1–49.
3. Naghmouchi I, Mutjé P, Boufi S. Polyvinyl chloride composites filled with olive stone flour: Mechanical, thermal, and water absorption properties. *Journal of Applied Polymer Science*. 2014;131(22):1–10. https://doi.org/10.1002/app.41083.
4. Ates M, Kuz P. Starch-based bioplastic materials for packaging industry. *Journal of Sustainable Construction Materials and Technologies*. 2020;5(1):399–406.
5. Menezes PL, Rohatgi PK, Lovell MR. Biomimetics, energy conservation and sustainability. In Studies on the tribological behavior of natural fiber reinforced polymer composite. *Green Tribology*. 2012. p. 329–345.
6. Potluri R, Chaitanya Krishna N. Potential and applications of green composites in industrial space. *Materials Today: Proceedings*. 2019;22:2041–2048. https://doi.org/10.1016/j.matpr.2020.03.218.
7. Väisänen T, Das O, Tomppo L. A review on new bio-based constituents for natural fiber-polymer composites. *Journal of Cleaner Production*. 2017;149:582–596. https://doi.org/10.1016/j.jclepro.2017.02.132.
8. Wang B, Zhan L, Guan C. Advanced polymer composites and applications. *Polymers*. 2025;17(15):2062. https://doi.org/10.3390/polym17152062.

9. Zandieh M, Griffiths E, Waldie A, Li S, Honek J, Rezanezhad F., *et al.* Catalytic and biocatalytic degradation of microplastics. *Exploration*. 2024;4(3):20230018.
10. Tang KHD, Lock SSM, Yap PS, Cheah KW, Chan YH, Yiin CL., *et al.* Immobilized enzyme/microorganism complexes for degradation of microplastics: A review of recent advances, feasibility and future prospects. *Science of the Total Environment*. 2022;832:154868. https://doi.org/10.1016/j.scitotenv.2022.154868.
11. Paxton NC, Allenby MC, Lewis PM, Woodruff MA. Biomedical applications of polyethylene. *European Polymer Journal*. 2019;118:412–428. https://doi.org/10.1016/j.eurpolymj.2019.05.037.
12. Omrani E, Menezes PL, Rohatgi PK. State of the art on tribological behavior of polymer matrix composites reinforced with natural fibers in the green materials world. *Engineering Science and Technology, an International Journal*. 2016;19(2):717–736. https://doi.org/10.1016/j.jestch.2015.10.007.
13. Balart JF, Fombuena V, Fenollar O, Boronat T, Sánchez-Nacher L. Processing and characterization of high environmental efficiency composites based on PLA and hazelnut shell flour (HSF) with biobased plasticizers derived from epoxidized linseed oil (ELO). *Composites Part B: Engineering*. 2015;86:168–177. https://doi.org/10.1016/j.compositesb.2015.09.063.
14. Banat R, Fares MM. Olive oil waste filled high-density polyethylene bio-composite: Mechanical, morphological and water absorption properties. *International Journal of Composite Materials*. 2015;5(5):133–141.
15. Bhowmik R, Das S, Mallick D, Gautam SS. Predicting the elastic properties of hemp fiber: A comparative study on different polymer composite. *Materials Today: Proceedings*. 2022;50:2510–2514. https://doi.org/10.1016/j.matpr.2021.09.562.
16. Devadiga, DG, Bhat KS, Mahesha GT. Sugarcane bagasse fiber reinforced composites: Recent advances and applications. *Cogent Engineering*. 2020;7(1):1823159. https://doi.org/10.1080/23311916.2020.1823159.
17. Al Rashid A, Khalid MY, Imran R, Ali U, Koc M. Utilization of banana fiber-reinforced hybrid composites in the sports industry. *Materials*. 2020;13(14):3167. https://doi.org/10.3390/ma13143167.
18. Sawalha SH, Ma'ali RA, Basheer DJ, Hussein RR, Abu-Zarour YN, Hamydeh LK. Mechanical and thermal properties of olive solid waste/recycled low-density polyethylene blends. *Journal of Scientific and Engineering Research*. 2018;5(4):268–275.
19. Ogah AO, Afiukwa JN. Characterization and comparison of mechanical behavior of agro fiber-filled high-density polyethylene bio-composites. *Journal of Reinforced Plastics and Composites*. 2014;33(1):37–46. https://doi.org/10.1177/0731684413509425.
20. Geckil T, Issi S, Ince CB. Evaluation of prina for use in asphalt modification. *Case Studies in Construction Materials*. 2022;17:e01623. https://doi.org/10.1016/j.cscm.2022.e01623.
21. Tasdemir M, Kastan A. Wear and mechanical properties of olive pit powder added polypropylene composite. *BEU Journal of Science*. 2021;10(2):568–576.
22. Memioglu F, Elibol M. Preparations and applications of bio-based additives for building chemicals production. *Journal of Sustainable Construction Materials and Technologies*. 2020;5(1):3379–3391.
23. Miranda I, Simões R, Medeiros B, Nampoothiri KM, Sukumaran RK, Rajan D., *et al.* Valorization of lignocellulosic residues from the olive oil industry by production of lignin, glucose and functional sugars. *Bioresource Technology*. 2019;292:121936. https://doi.org/10.1016/j.biortech.2019.121936.
24. Gómez-Cruz I, del Mar Contreras M, Romero I, Castro E. Towards the integral valorization of olive pomace-derived biomasses through biorefinery strategies. *ChemBioEng Reviews*. 2024;11(2):253–277.
25. Ameziane H, Mabrouki J, Benchrifha M, Hmouni D. Review of olive pomace valorization techniques: A sustainable perspective for the olive oil industry. In *Advanced technology for smart environment and energy*. Springer Berlin, Heidelberg; 2024; p. 165–183.
26. Jurado-Contreras, S, Navas-Martos FJ, Rodríguez-Liébana JA, Moya AJ, de la Rubia MD. Manufacture and characterization of recycled polypropylene and olive pits biocomposites. *Polymers*. 2022;14(19):4206. https://doi.org/10.3390/polym14194206.
27. Baysal A, Yayla P, Trükmen HS. A review on engineering biocomposites and natural fiber-reinforced materials. *Journal of Sustainable Construction Materials and Technologies*. 2022;7(3):231–249.
28. Alfaifi HY, Aldress SD, Alshammari BA. Exploitation of plastic and olive solid wastes for accelerating the biodegradation process of plastic. *Journal of Composites Science*. 2025;9(8):445. https://doi.org/10.3390/jcs9080445.
29. Djidjelli H, Benachour D, Boukerrou A, Zefouni O, Martinez-Véga J, Farenc J., *et al.* Thermal, dielectric and mechanical study of poly(vinyl chloride)/olive pomace composites. *Express Polymer Letters*. 2007;1(12):846–852.
30. Gümüs BE, Yagci O, Erdogan DC, Tasdemir M. Dynamical mechanical properties of polypropylene composites filled with olive pit particles. *Journal of Testing and Evaluation*. 2019;47(4):2551–2561. https://doi.org/10.1520/JTE20180198.
31. Kiliçaslan C. Determination of mechanical properties of olive residue/polyester composite under compressive loading. *Mühendis ve Makina*. 2016;57(676):26–31.
32. Hamida B, Ahmed M, Nadia N, Samira M, June M, June M. Mechanical properties of polystyrene/olive stone flour composites. *Research Journal of Pharmaceutical, Biological and Chemical Sciences*. 2015;6(3):127–132.
33. Pickering KL, Efendy MGA, Le TM. A review of recent developments in natural fibre composites and their mechanical performance. Composites Part A: Applied Science and Manufacturing. 2016;83:98–112.
34. Rohit K, Dixit S. A review—Future aspect of natural fiber reinforced composite. *Polymers from Renewable Resources*. 2016;7(2):43–59.
35. Dunne R, Desai D, Sadiku R, Jayaramudu J. A review of natural fibres, their sustainability and automotive applications. *Journal of Reinforced Plastics and Composites*. 2016;35(13):1041–1050.
36. Banat R. Olive pomace flour as potential organic filler in composite materials: A brief review. *American Journal of Polymer Science*. 2019;9(1):10–15.
37. Gullon P, Gullon B, Astray G, Carpena M, Fraga-Corral M, Prieto MA., *et al.* Valorization of by-products from olive oil industry and added-value applications for innovative functional foods. *Food Research International*. 2020;137:109683.
38. Benarab A, Blazquez-Blazquez E, Krache R, Benavente R, Cerrada ML, Perez E. Composites of a polypropylene random copolymer and date stone flour: Crystalline details and mechanical response. *Polymers*. 2021;13:2957.
39. Moubarik A, Grimi N. Valorization of olive stone and sugar cane bagasse by-products as biosorbents for the removal

of cadmium from aqueous solution. *Food Research International*. 2015;73:169–175. https://doi.org/10.1016/j.foodres.2014.07.050.
40. Valvez S, Maceiras A, Santos P, Reis PNB. Olive stones as filler for polymer-based composites: A review. *Materials*. 2021;14:845.
41. Koutsomitopoulou AF, Bénézet JC, Bergeret A, Papanicolaou GC. Preparation and characterization of olive pit powder as a filler to PLA-matrix bio-composites. *Powder Technology*. 2014;255:10–16. https://doi.org/10.1016/j.powtec.2013.10.047.
42. ASTM D4442M-20. Standard test methods for direct moisture content measurement of wood and wood-base materials. ASTM International; 2020.
43. ISO 527-2. Plastics—Determination of tensile properties—Part 2: Test conditions for moulding and extrusion plastics. International Organization for Standardization; 2025.
44. ASTM D792-20. Standard test methods for density and specific gravity (relative density) of plastics by displacement. ASTM International; 2020.
45. ASTM D2240-15. Standard test method for rubber property—Durometer hardness. ASTM International; 2021.
46. ASTM D570-98. Standard test method for water absorption of plastics. ASTM International; 2018.
47. ISO 179-1. Plastics—Determination of Charpy impact properties—Part 1: Non-instrumented impact test. International Organization for Standardization; 2023.
48. Oliveros-Gaviria C, Cumbalaza E, Mina-Hernandez JH, Valencia-Zapata ME, Suarez-Bonilla JN, Martinez-Mera N. Wood plastic composite based on recycled high-density polyethylene and wood waste (sawdust). *Polymers*. 2024;16(22):3136. https://doi.org/10.3390/polym16223136.
49. Kuzmin A, Ashori A, Pantyukhov P, Zhou Y, Guan L, Hu C. Mechanical, thermal, and water absorption properties of HDPE/barley straw composites incorporating waste rubber. *Scientific Reports*. 2024;14(1):1–11. https://doi.org/10.1038/s41598-024-76337-6.
50. Tuna S, Sen I. Characterization of olive seed powder incorporated low-density polyethylene composites. *Sakarya University Journal of Science*. 2025;29(1):71–82. https://doi.org/10.16984/saufenbilder.1589003.
51. Anaç N, Temiz A, Koçar O, Güldibi AS. Production of biocomposites with hazelnut shell and pomace additives by plastic injection molding. *International Journal of Pure and Applied Sciences*. 2024;10(1):72–88.
52. Mohammed M, Rasidi MSM, Mohammed AM, Rahman R, Osman AF, Adam T., *et al.* Interfacial bonding mechanisms of natural fibre-matrix composites: An overview. *BioResources*. 2022;17(4):7031–7090.
53. Magalhães WLE, Pianaro SA, Granado CJF, Satyanarayana KG. Preparation and characterization of polypropylene/heart-of-peach palm sheath composite. *Journal of Applied Polymer Science*. 2013;127(2):1285–1294. https://doi.org/10.1002/app.37633.
54. Kaya N, Atagur M, Akyuz O, Seki Y, Sarikanat M, Sutcu M., *et al.* Fabrication and characterization of olive pomace filled PP composites. *Composites Part B: Engineering*. 2018;150:277–283. https://doi.org/10.1016/j.compositesb.2017.08.017.
55. Sheikh TZ, Mozumdar FA, Karim MR, Ahsan Q. Investigation of mechanical, morphological and thermal properties of waste glass powder and wood flour reinforced polypropylene composite. *Heliyon*. 2025;11(1):e41352. https://doi.org/10.1016/j.heliyon.2024.e41352.
56. Aliotta L, Gigante V, Cinelli P, Coltelli MB, Lazzeri A. Effect of a bio-based dispersing aid (EINAR®101) on PLA-Arbocel®biocomposites: Evaluation of the interfacial shear stress on the final mechanical properties. *Biomolecules*. 2020;10(11):1–19.
57. Lee CH, Khalina A, Lee SH. Importance of interfacial adhesion condition on characterization of plant-fiber-reinforced polymer composites: A review. *Polymers*. 2021;13(3):1–22.
58. Le Moigne N, Longerey M, Taulemesse JM, Bénézet JC, Bergeret A. Study of the interface in natural fibres reinforced poly(lactic acid) biocomposites modified by optimized organosilane treatments. *Industrial Crops and Products*. 2014;52:481–494. https://doi.org/10.1016/j.indcrop.2013.11.022.
59. Arrakhiz FZ, El Achaby M, Malha M, Bensalah MO, Fassi-Fehri O, Bouhfid R., *et al.* Mechanical and thermal properties of natural fibers reinforced polymer composites: Doum/low-density polyethylene. *Materials & Design*. 2013;43:200–205. https://doi.org/10.1016/j.matdes.2012.06.056.
60. Lazrak C, Kabouchi B, Hammi M, Famiri A, Ziani M. Structural study of maritime pine wood and recycled high-density polyethylene (HDPEr) plastic composite using infrared-ATR spectroscopy, X-ray diffraction, SEM and contact angle measurements. *Case Studies in Construction Materials*. 2019;10:e00227. https://doi.org/10.1016/j.cscm.2019.e00227.
61. Tarani E, Arvanitidis I, Christofilos D, Bikiaris DN, Chrissafis K, Vourlias G. Calculation of the degree of crystallinity of HDPE/GNPs nanocomposites by using various experimental techniques: A comparative study. *Journal of Materials Science*. 2023;58(4):1621–1639. https://doi.org/10.1007/s10853-022-08125-4.
62. Zerbi G, Gallino G, Del Fanti N, Baini L. Structural depth profiling in polyethylene films by multiple internal reflection infra-red spectroscopy. *Polymer*. 1989;30(12):2324–2327. https://doi.org/10.1016/0032-3861(89)90269-3.
63. Bootkul D, Raksanti A, Intarasiri S. Investigation on the application of coconut copra residue for the reinforcement of high-density polyethylene composites. *Discover Applied Sciences*. 2026;8(3):279.
64. Lipska K, Betlej I, Rybak K, Nowacka M, & Boruszewski P. Oil plant pomace as a raw material in technology of sustainable thermoplastic polymer composites. *Sustainability*. 2024;16:7088.
65. Aslan Türker D, Işçimen EM. Insoluble dietary fiber and microparticle formation from olive pomace: Effects on emulsification and interfacial behavior in Pickering emulsions. *Journal of Food Measurement and Characterization*. 2025;19(4):2684–2699. https://doi.org/10.1007/s11694-025-03139-3.
66. Sánchez-Ávila N, Carmona-Cabello M, Cano-Galey M, Romero PE, Dorado MP. Olive pomace as a reinforcing agent in PETG filaments for 3D printing in the context of circular economy. *Materials Circular Economy*. 2025;7(1). https://doi.org/10.1007/s42824-025-00186-5.
67. Oulidi O, Nakkabi A, Elaraaj I, Fahim M, El Moualij N. Incorporation of olive pomace as a natural filler into the PA6 matrix: Effect on the structure and thermal properties of synthetic polyamide 6. *Chemical Engineering Journal Advances*. 2022;12:100399. https://doi.org/10.1016/j.ceja.2022.10039.